

1 of 1



IS-5100
UC-700
UC-515

AMES LABORATORY

OPTICAL ASSAY TECHNOLOGY FOR SAFEGUARDS

Quarterly Report
January 1 - March 31, 1992

M.C. EDELSON, S.C. LEE, R.J. LIPERT, G.M. MURRAY,
R.A. SCHULER, S.J. WEEKS, and Z-M. WANG

Prepared for the Office of Safeguards and Security

Date Transmitted: May 1993

Ames Laboratory
Iowa State University
Ames, Iowa 50011

Prepared for
The U.S. Department of Energy
under contract W-7405-eng-82

MASTER

DISCLAIMER

This report was prepared as an account of work sponsored by an agency of the United States Government. Neither the United States Government nor any agency thereof, nor any of their employees, makes any warranty, express or implied, or assumes any legal liability or responsibility for the accuracy, completeness or usefulness of any information, apparatus, product, or process disclosed, or represents that its use would not infringe privately owned rights. Reference herein to any specific commercial product, process, or service by trade name, trademark, manufacturer, or otherwise, does not necessarily constitute or imply its endorsement, recommendation, or favoring by the United States Government or any agency thereof. The views and opinions of authors expressed herein do not necessarily state or reflect those of the United States Government or any agency thereof.

Printed in the United States of America

Available from
National Technical Information Service
U.S. Department of Commerce
5265 Port Royal Road
Springfield, VA 22161

TABLE OF CONTENTS

TABLE OF CONTENTS	ii
ABSTRACT	iii
INTRODUCTION	1
RESEARCH SUMMARY	
1. INDUCTIVELY COUPLED PLASMA - LASER EXCITED ATOMIC FLUORESCENCE SPECTROSCOPY (ICP-LEAFS)	1
2. SAFEGUARDS FOR LASER ISOTOPE ENRICHMENT FACILITIES	4
3. APPLICATIONS OF DIODE LASERS	7
DISTRIBUTION LIST	15

sp
DISTRIBUTION OF THIS DOCUMENT IS UNLIMITED

ABSTRACT

Research conducted in the Ames Laboratory Nuclear Safeguards and Security Program during the period January 1, 1992 to March 31, 1992 is reviewed. Work in applying optical spectroscopy to the determination of actinides and related elements in the gas phase is discussed. The application of diode lasers to the measurement of an actinide (U) and the rare-earth elements by optogalvanic spectrometry is discussed.

INTRODUCTION

The concept of using optical spectrometry to measure the abundance of actinide elements is novel to many in the nuclear community. Work in this program at the Ames Laboratory is continuing to develop optical spectroscopy for such measurements. The major portion of this report is devoted to a description of recent investigations, involving laser spectroscopy, which will result in a system capable of quantitative, real-time measurements of actinides and isotopic ratios of actinides being enriched by laser enrichment methods.

1. INDUCTIVELY COUPLED PLASMA - LASER EXCITED ATOMIC FLUORESCENCE SPECTROSCOPY (ICP-LEAFS)

Purpose:

To assess the feasibility of ICP-LEAFS for the determination of Pu and its isotopes without the need for chemical separations from matrix elements or the oxidation state adjustment of Pu prior to analysis.

Progress:

At the beginning of this quarter all Ames Laboratory Class IV laser operations were suspended until door interlocks were installed on laser laboratories. This, as well as new training requirements and other preparations for and during the Tiger Team inspection, interfered with ICP-LEAFS experimentation. Attention was shifted toward discovering which atoms could be determined by ICP-LEAFS using the current instrumentation. Table 1 lists twenty elements that should be measurable with the current ICP-LEAFS instrumentation. Several of the elements have more than one transition for which direct line fluorescence with reasonable intensity will occur. Those elements whose emission column entry is blank require monitoring resonant fluorescence or finding a thermally assisted fluorescence line. Of particular significance to Safeguards concerns are thorium, lead and several lanthanides.

Due to safety concerns it was necessary to totally enclose the laser beam path for ICP-LEAFS. This was accomplished using an opaque plastic enclosure. The enclosure for the frequency doubler required removal when changing wavelengths to permit retuning of the doubler crystal. At the end of the quarter, door interlocks were installed and laser experimentation was allowed to proceed. The four days remaining in the quarter were used to investigate ICP-LEAFS of lead. It was hoped that isotopic structure might be resolved for one hyperfine component of ^{207}Pb , which is split about 10 GHz or 2 pm from the $^{208}\text{-}^{206}\text{Pb}$ line for the 283.306 nm Pb transition. The expected Doppler width of lead at this frequency was 0.56 pm, suggesting that the hyperfine component could be resolved. Since the aforementioned line is an atom line and not an ion line, plasma conditions needed to be modified to produce a cooler plasma. This was done by using an auxiliary gas flow of 2.0 L/min and adjusting the gas flow for the nebulizer until it was just off scale (>1.1 L/min). After a considerable amount of adjustment of the dye laser aided by the new wavemeter the spectrum presented below as Figure 1 was obtained.

Table 1.
Elements Suitable for Study with ICP-LEAFS and Useful Transitions for Monitoring

Element	Excitation Intensity λ(nm)	Energy Levels (cm ⁻¹)	Emission Intensity λ(nm)	Energy Levels (cm ⁻¹)
Ba(II)	585.368	2800 4874-21952	614.172	20000 5675-21952
Bi(I)	289.798	4000 11418-45915	412.153	140 21660-45915
Cr(II)	284.325	1700 12304-47465	285.891	610 12497-47465
Eu(II)	290.668	3200 0-34394	305.494	320 1669-34394
Eu(II)	281.394	3400 0-35527	295.268	200 1669-35527
Eu(II)	282.078	2000 0-35441	296.021	260 1669-35441
Ga(I)	287.424	5000 0-34782	294.418	1500 826-34782
Hf(II)	282.022	1200 3051-38499	310.912	710 6344-38499
Ir(I)	284.972	3800 0-35081	357.372	1200 7107-35081
Lu(II)	289.484	6300 14199-48733	275.417	3600 12435-48733
Lu(II)	284.751	3000 11796-46904	290.030	4500 12435-46904
Mg(I)	285.213	60000 0-35051		
Mo(II)	284.823	1700 12900-47999	289.445	950 13461-47999
Mo(II)	287.151	1700 12417-47232	291.192	1100 12900-47232
Pb(I)	283.306	9500 0-35287	405.783	34000 10650-35287
Pb(I)	280.199	10000 10650-46329	401.964	400 21458-46329
Sb(I)	287.792	1400 8512-43249	231.147	2200 0-43249
Si(I)	288.160	260 6299-40992	390.553	11 15394-40992
Sn(I)	283.999	14000 3428-38629	270.651	7000 1692-38629
Sn(I)	286.333	10000 0-34914	300.914	7000 1692-34914
Ta(II)	285.098	1900 14581-49647	221.019	1400 4416-49647
Th(II)	283.231	800 4147-39443	343.971	530 10379-39443
Th(II)	283.730	1200 6214-41448		
Th(II)	287.041	550 1860-36688		
U(II)	286.568	970 0-34886	288.963	1200 289-34886
V(II)	290.882	2400 3163-37531	268.796	1100 339-37531
Yb(II)	289.138	3600 0-34575		
Zr(I)	283.723	710 570-35806	289.226	120 1241-35806
Zr(I)	283.723	710 570-35806	279.204	120 0-35806
Zr(II)	284.458	660 8056-43202	258.340	75 4506-43202

The peak in Figure 1 is asymmetric due to isotope and hyperfine structure and the inflection at about 2 pm from the unresolved ^{208}Pb - ^{206}Pb peak is likely due to ^{207}Pb . Although curve-fitting techniques could be used to deconvolve the spectrum, the resolution is too poor to allow routine isotopic analysis using this line. Attempts to further tune the dye laser resulted in a loss of the inflection and it appears that the resolution of the isotopes is dye laser limited. Unfortunately, in the case of lead, there are no usable transitions in the fundamental region of the dye laser so the reduced laser linewidth obtainable in that region could not be exploited. Since isotopic resolution wasn't feasible, the filter that reduces the energy of the pump laser to the oscillator was removed. This increases dye laser power and results in better limits

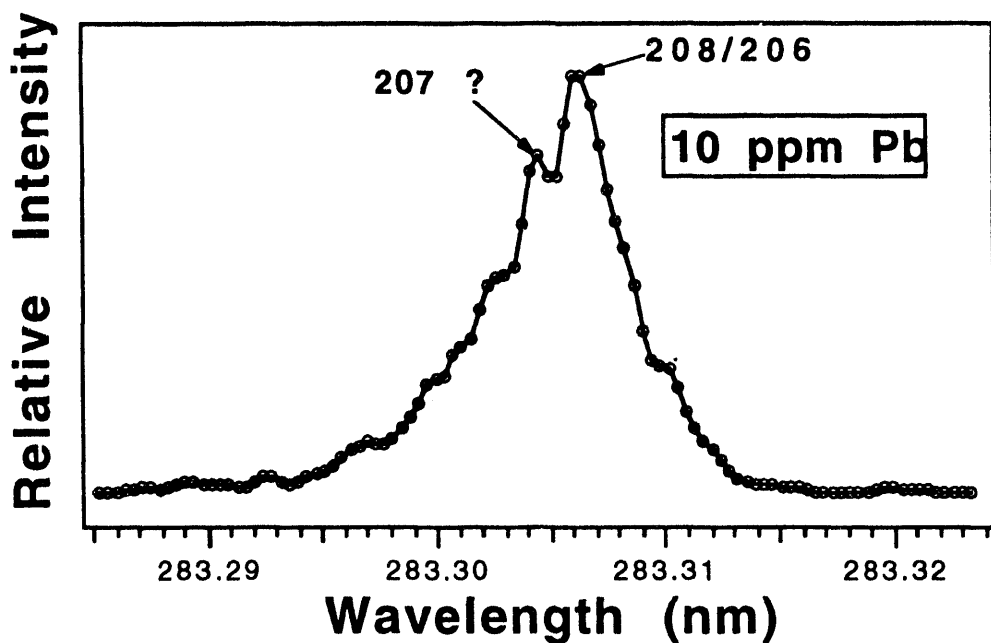


Figure 1. ICP-LEAFS excitation spectrum of lead (emission wavelength 405.783 nm; data smoothed).

of detection. Using the conditions stated above, we proceeded to determine the analytical figures of merit for ICP-LEAFS of lead. Two of the spectra obtained in this process are presented in Figure 2. The limit of detection for lead was reasonably good, 2 ppb. The reason that this is so much better than our limit of detection for uranium is because of the high intensity of the transitions monitored. This is true even though these are atom lines and not ion lines. Pumping the oscillator with greater power is seen to reduce resolution relative to that shown in Figure 1.

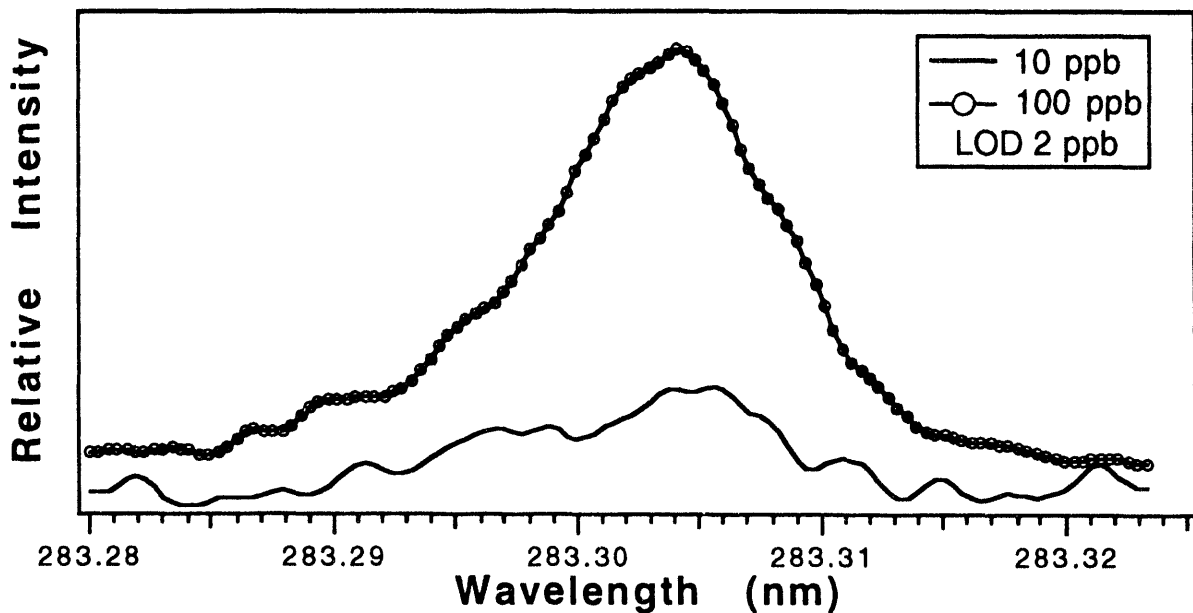


Figure 2. ICP-LEAFS spectra of lead under conditions optimized for high sensitivity.

2. SAFEGUARDS FOR LASER ISOTOPE ENRICHMENT FACILITIES

Most of the activities of this quarter involved the preparation for, and response to, a Tiger Team visit. The most dramatic impact was that all high-powered lasers were shut down until an interlock system for the laboratory was installed. The shut down occurred early in the quarter and lasted for the duration. Therefore, no high-resolution spectroscopic work could be performed with the ring dye laser system. However, it was possible to operate the diode laser system (another good reason for moving toward the use of diode lasers) and some experiments using the diode laser to investigate materials in an atomic beam were performed. Also, some studies were made of atomic and ionic emission above the electron gun.

Atomic And Ionic Emission Above The Electron Gun Evaporation Source

Purpose:

It is well known that an electron gun vaporization source, like the one we are using in the atomic beam experiments, produces electronically excited atoms and ions. In a low pressure environment these excited species emit light as they return to lower energy levels. Thus, there is the potential for monitoring the vapor composition by simply monitoring the emission excited by electron impact. We began exploring this possibility in the fourth quarter of FY-1991 by examining the emission generated when yttrium and gadolinium were vaporized in the atomic beam apparatus. This work was continued in this quarter.

Progress:

We continued to study gadolinium emission from a region roughly 12 mm above a molten sample. Gadolinium was chosen as a test atom because of its isotopic composition (see April-June 1991 Quarterly Report). Of its three naturally occurring isotopes, gadolinium has three even mass number isotopes present at roughly 16%, 22%, and 25% levels. These isotopes dominate the isotopically resolved spectra of gadolinium. The isotope splittings for these components are roughly 1 GHz, which is a little less than the maximum resolution of our high-resolution monochromator. Still, it was hoped that some structure would be evident in the spectra.

The gadolinium emission was coupled into a fiber optic cable with a 10X microscope objective, having a numerical aperture of 0.25, located 18 cm from the source. The light exiting the fiber was f-matched into a 1.5 m monochromator (f/12) equipped with a 3600 groove/mm grating and used in double-pass mode. Light was detected at the exit slit with a cooled EMI 9804QA photomultiplier and photon counting electronics. The signal proved to be weak so it was not possible to operate the monochromator at its maximum resolution. This was due, in part, to the window on the vaporization chamber becoming coated with gadolinium during the data collection.

The wavelength of the spectra were calibrated using a thorium hollow cathode lamp and an atlas of thorium hollow cathode emission lines (Byron A. Palmer and Rolf Engleman, Jr. "Atlas of the Thorium Spectrum," LANL Rep. LA-9615). The thorium emission was directed through the vacuum chamber so that the gadolinium and thorium spectra could be collected simultaneously.

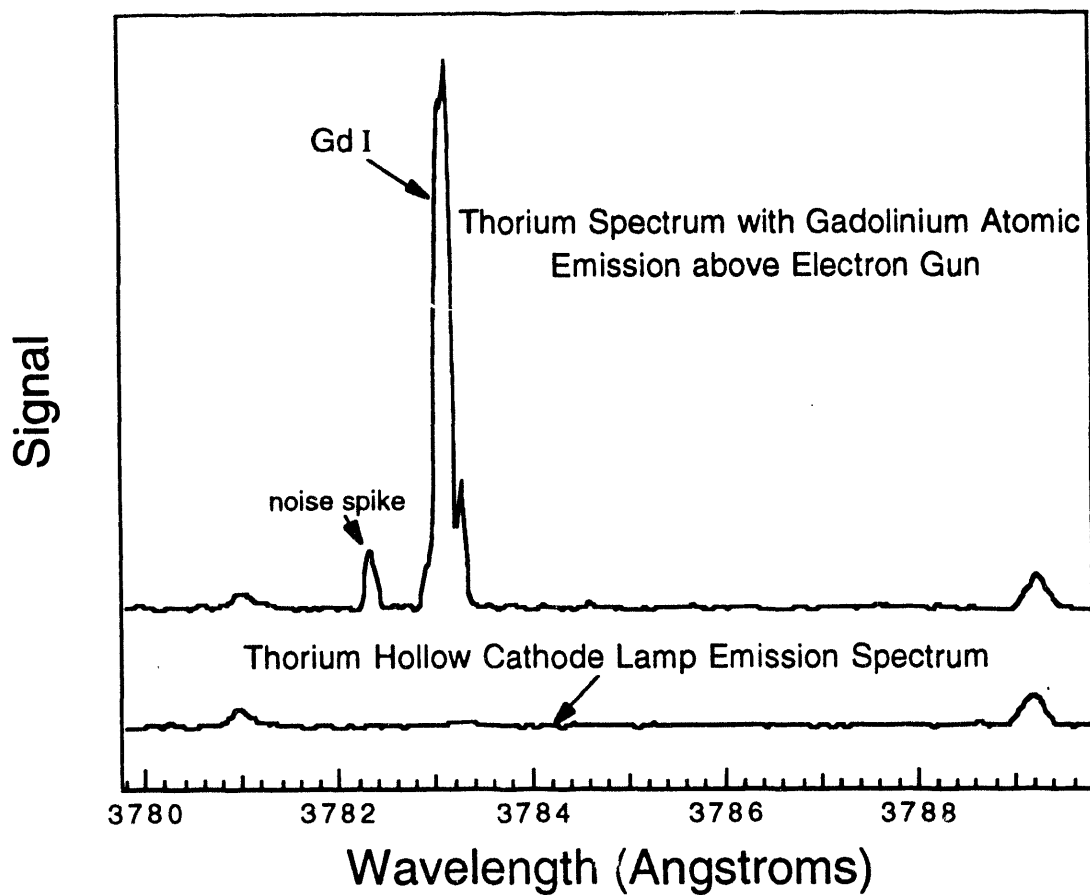


Figure 3. Emission spectrum of neutral gadolinium vaporized by an electron gun.

Figure 3 shows a portion of the gadolinium spectrum in the region of the 378.305 nm neutral line. The spectrum is from a region roughly 12 mm above the molten sample. The lower trace was taken with the electron gun turned off; all peaks are due to a reference thorium hollow cathode lamp. The upper trace was obtained with both the hollow cathode and the electron gun running. The spectra have been smoothed twice with a binomial smoothing algorithm.

The Gd line observed in Figure 3 is the second strongest neutral line in the d-c arc spectra of Meggers et al. (W.F. Meggers, C.H. Corliss, B.F. Scribner, "Tables of Spectral-Line Intensities Part I," NBS Monograph 145). The apparent structure on the strong peak is not due to individual isotopes but to signal variations. To produce a strong signal, the electron gun was operated at 250 mA. This is a relatively high current level (roughly 70 mA are required to melt gadolinium). At this level the gun was unstable and produced strongly varying signals. Because of this instability, it appears unlikely that we will be able to obtain quantitative results for such parameters as isotope ratios with the current experimental setup.

We were also curious to see if enough ions are being produced by the electron gun for them to be detected in this setup. Figure 4 shows a region of the spectrum containing the strongest ion line (in the d-c arc) at 376.839 nm.

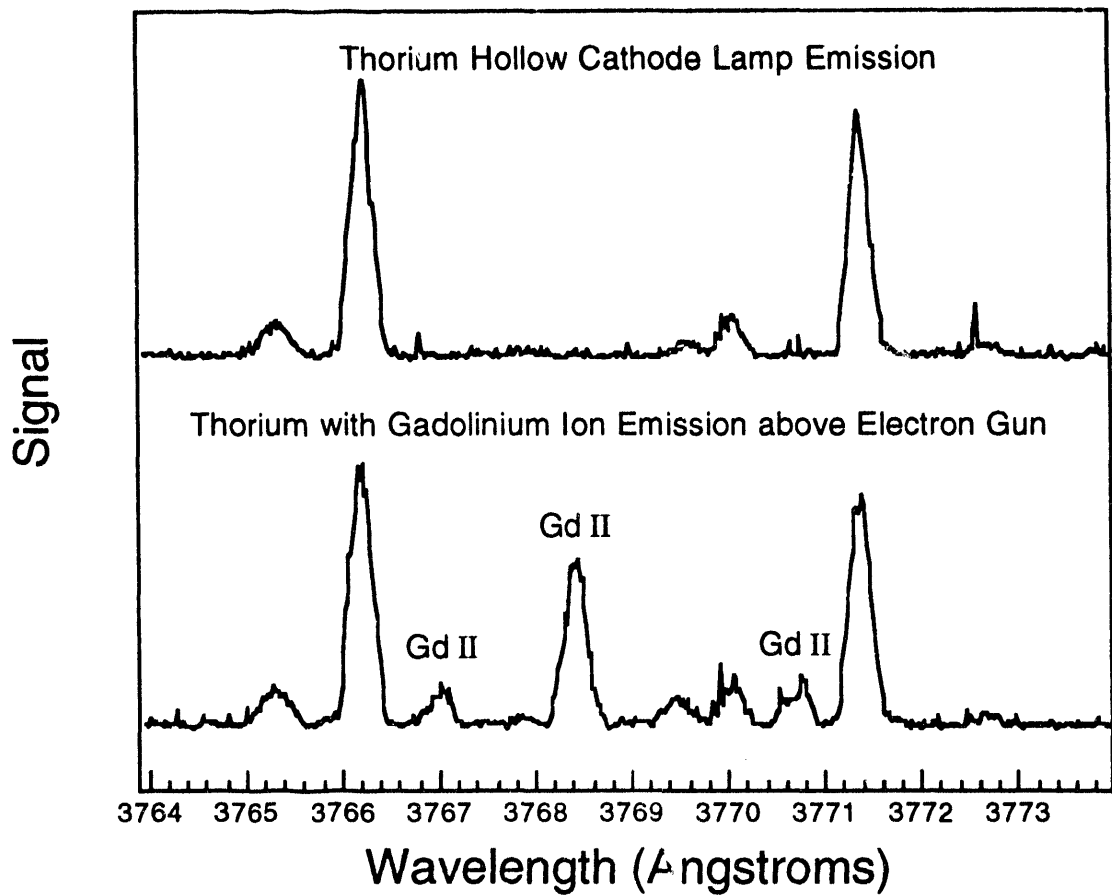


Figure 4. Emission spectra above the electron gun vaporizer showing gadolinium ion emission lines. The top trace is of the reference thorium hollow cathode alone. The lower trace is a repeat of the same scan with the electron gun turned on. These spectra were not smoothed.

Three ion lines are clearly visible. The Einstein coefficient for spontaneous emission for the line at 376.839 nm is roughly half that of the neutral line shown in Fig. 3. In our spectra the neutral line is about ten times stronger than this ion line. This shows, very roughly, that there is five times as much neutral gadolinium as singly ionized gadolinium in this region above the electron gun.

Future Studies:

It is difficult to perform isotopic abundance measurements in the plasma formed by the electron gun vaporization source. The primary obstacles are low signal levels, signal instability at electron gun currents necessary to produce adequate signal, and loss of spectral resolution due to Zeeman splitting of the spectra by the magnets of the electron gun. It might be possible to use lower resolution emission data to normalize laser excited fluorescence spectra and correct for fluctuations in the atomic beam intensity. This data can be collected at lower electron gun currents where the gun is more stable.

3. APPLICATIONS OF DIODE LASERS

Purpose:

Optical absorption spectroscopy has recently been applied to the measurement of Pu in fuel dissolver solutions (Kuno, et al., "Input Plutonium Accountability Analysis in a Reprocessing Plant by Spectrophotometry Using Internal Standards," Proc. 31st INMM Annual Meeting, July 15-18, 1990, pgs. 817-821). No chemical separation of Pu from U was required. This measurement, achieved with non-laser light sources, was not capable of isotopic resolution. It required relatively concentrated solutions (only a factor of 20 dilution of dissolver solution with ~ 1g/L Pu was used) that have the potential of damaging the quartz optical absorption cell through the formation of radiation-induced color centers.

This work investigates the application of diode lasers to the real-time, optical spectroscopic measurement of actinides. Laser-based optical spectroscopy can result in improved detection limits, which permit the use of lower analyte concentrations, and isotopic selectivity. Diode lasers confer additional advantages: low cost, ease of use, narrow single-mode line widths, and wavelength tunability. It is also notable that most actinides have a rich spectrum with transitions from low-lying levels occurring in the red and near-infrared regions of the spectrum. These wavelengths can be reached with well-developed AlGaInP and AlGaAs laser diodes. The shortcomings of the diode laser, e.g., mode hops, low power, and narrow wavelength range coverage, still limit the application of diode lasers. A diode laser system with fiber optics is being developed for the real-time, remote monitoring of radioactive materials for field and on-site measurements.

Progress:

The modular diode laser system, which consisted of four separate units: the diode laser unit, the beam monitoring unit, the sampling unit, and the data acquisition unit, was improved this quarter by installing an ultra low noise power supply (Seastar Model LD-2000), a low noise thermoelectric (TE) temperature controller (Seastar Model TC-5100), and a picowatt digital power meter (Newport Model 835). The diode laser driver has a stability of 2 ppm (short term) and root-mean square ripple of less than 750 mA; the temperature controller has a stability of +/- 0.01 °C and a precision of +/- 0.02 °C. These components delivered at least ten times better stability than the components that they replaced. In-house software, written in Turbo Pascal, is used to scan the diode laser, collect signals from a lock-in amplifier, and read the wavemeter. Precision diode laser wavelength scanning was achieved by adding a controlled DC voltage from the lock-in amplifier to the external DC voltage input of the diode laser power supply. This scanning method improved the accuracy and reproducibility of recorded spectra. We began the construction of an Electrothermal Hollow Cathode Discharge Spectrometer (ET-HCDS) this quarter. This device combines the techniques of graphite furnace atomization and glow discharge spectrometry and will be used with the diode laser system for measurements of actinides, their isotopes, and rare earth elements.

About 52 elements have one or more sensitive transition(s) in the wavelength region spanned by commercial diode lasers. Among them, 22 elements have strong

transitions that should be easily observable with conventional diode lasers. Another 17 elements have relatively weak transition(s) that should still be detectable with diode lasers. The remaining 13 elements can only be detected with frequency doubled diode lasers. The elements having strong transitions accessible with diode lasers are listed in Table 2 along with proposed monitoring lines. Lines for other elements are summarized in Table 3.

Table 2. Selected elements that should have intense spectral lines (i.e., high transition probabilities) in the wavelength range spanned by commercial laser diodes.

Element	Ion Status	Observed Lines (nm)	Transition(s) (cm ⁻¹)	Relative Intensity ^a
Cs	I	698.349*	11732-->26048	35
	I	852.124	0-->11732	15000
	I	894.359	0-->11178	8000
Dy	I	683.542	0-->14625	180
	II	353.170*	0-->28306	22000
	II	820.157	16117-->28306	100
Er	I	660.111	17073-->32218	70
	I	840.999	0-->11887	55
	I	847.242	0-->11799	35
	II	326.478*	0-->30621	2700
Eu	II	381.967*	0-->26173	39000
	I	686.454	0-->14564	360
Gd	I	673.073	999-->15852	85
	I	682.825	533-->15174	100
	I	773.350	999-->13926	80
	II	366.460*	7992-->35272	2700
	II	663.436	10600-->25669	35
La	II	677.426	1016-->15774	120
	I	670.950	3010-->17910	180
Li	I	670.784	0-->14940	36000
Nb	I	460.677*	2805-->24507	1200
	I	666.084	9498-->24507	210
	I	667.733	9043-->24015	150
	I	672.362	8705-->23574	130
K	II	766.490	0-->13043	18000
	I	769.896	0-->12985	9000

Pr		405.486*	1744-->26398	2200
		667.378	11419-->26398	75
		406.283*	3403-->28010	3400
		667.341	13029-->28010	55
		405.653*	5079-->29724	2200
		665.683	14706-->29724	75
		679.860	8080-->22785	55
Pu		820.930	0-->12178	**
Rb		780.023	0-->12817	30000
		794.760	0-->12579	15000
Sm		673.184	9407-->24257	120
		439.086*	1489-->24257	1600
		792.814	12988-->25598	90
		443.432*	3053-->25598	1800
Ag		768.787	29552-->42556	320
		827.352	30473-->42556	500
Na		818.326	16956-->29173	1100
		819.482	16973-->29173	2200
Sr		661.726	18159-->33267	300
		679.105	14218-->29039	180
		687.838	14504-->29039	480
Ta		661.195	11241-->26364	110
		667.373	9759-->24739	100
		667.553	11244-->26220	180
		681.325	9253-->23927	160
		686.623	12235-->26795	210
		788.237	11244-->23927	100
		828.162	9976-->22047	75
Tb		679.458	11261-->25975	130
		384.873*	0-->25975	3700
		819.482	13605-->25804	65
		387.417*	0-->25804	3500
Tm		660.496	17346-->32479	95
		773.153	19548-->32479	80
		793.084	19753-->32359	110

Ti	I	674.312	7255-->22081	80
		797.888	15220-->27750	60
		837.785	6661-->18594	100
		838.254	6599-->18525	100
		841.236	6599-->18483	120
		842.652	6661-->18525	170
		843.494	6843-->18695	490
		843.570	6743-->18594	240
		867.539	8602-->20126	90
Y	II	661.375	14098-->29214	95
	II	360.073*	1450-->29214	10000
	I	668.758	0-->149491	150
	I	670.071	18512-->33432	70
	II	679.541	14018-->28730	70
	II	361.105*	1045-->28730	7800
	II	788.190	14833-->27517	110
	II	363.312*	0-->27517	7800
	I	880.062	0-->11360	95
U	I	682.693	0-->14644	90
	I	778.416	620-->13463	14
	I	844.535	3801-->15638	35
	I	860.796	0-->11614	75

^a These values were referenced by W.F. Meggers, C.H. Corliss, and B.F. Scribner, "Tables of Spectral-Line Intensities, Part I," NBS Monograph, 1975.

* These lines can be used for non-resonance laser induced fluorescence detection.

** The data were not compatible with data from the NBS Monograph.

Table 3. List of elements that have weak transitions in the fundamental wavelength region of commercial diode lasers and relatively strong transitions in the wavelength region of frequency doubled diode lasers.

Weak Spectral Transitions	Strong Spectral Transitions
Be, Ca, Cu, Hf, Ho, Lu, Mg, Nd, Pd, Pt, Re, Ru, Sc, Se, Th, V	Ce, Cr, Co, Ga, In, Fe, Pb, Hg, Nd, Os, Rh, Th, W

Optogalvanic Spectroscopy

Doppler-limited optogalvanic spectroscopy of uranium, thorium, and rubidium in commercial hollow cathode tubes was reinvestigated with the improved diode laser system. Doppler limited environment in the sealed hollow cathode lamp was not suitable to investigate the hyperfine structures of metal atoms. Two peaks from U atom are observed with smooth wavelength scanning of the AlGaAs diode laser. These transitional bands are relatively weak but are still detectable with a reasonable S/N ratio. The spectrum is shown in Figure 5.

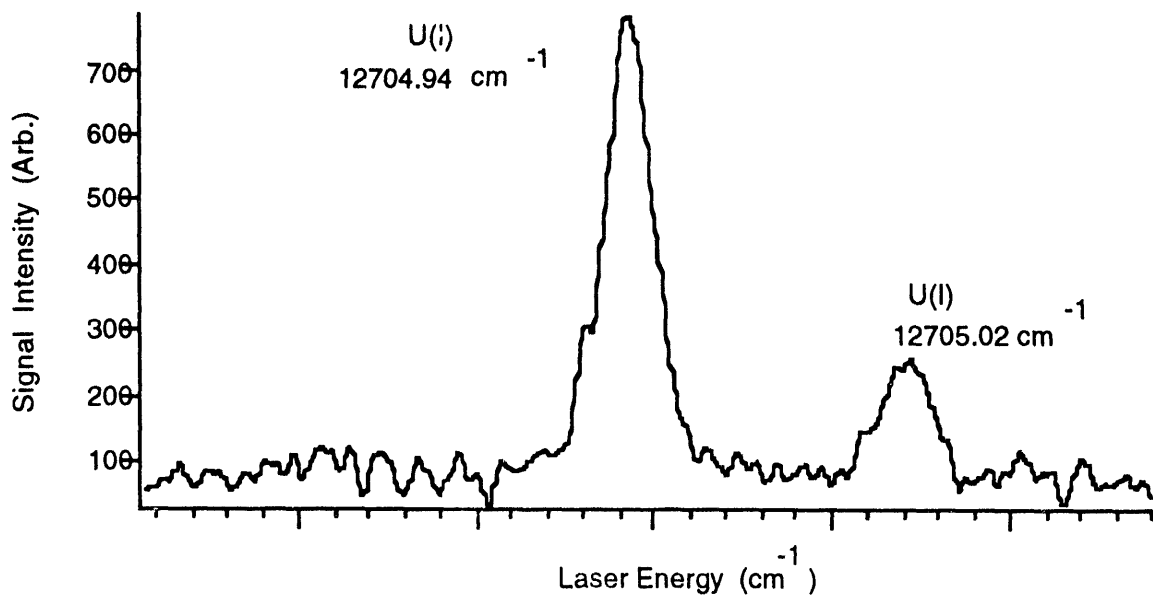


Figure 5. Diode laser optogalvanic spectrum of uranium in a hollow cathode lamp.

In this report, we add the diode laser optogalvanic spectrum of the rubidium D2 line (780.023 nm) in which the hyperfine splittings of rubidium were observed. The Rb spectrum is shown in Figure 6. Ground state notations(e.g., F values) are used in the spectrum. Two other Rb lines at 775.765 nm and 775.943 nm were detected but hyperfine splittings were not detectable.

The observed transitional lines of uranium, thorium, and rubidium in the commercial hollow cathode lamps are summarized in Table 4.

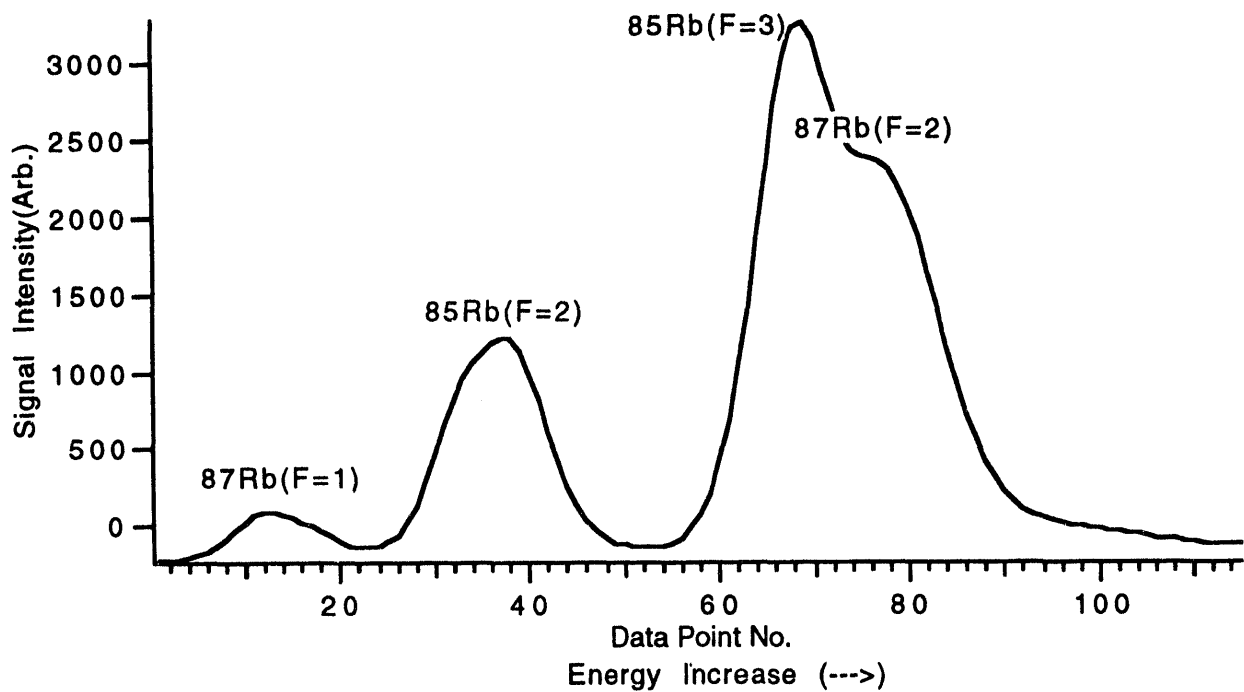


Figure 6. Diode laser optogalvanic spectrum of rubidium in a hollow cathode lamp. The hyperfine structure is mainly due to the ground state splittings of each isotope.

Table 4. Atomic spectral lines observed by optogalvanic detection using diode laser sources.

Element	Observed Lines (nm)	Transitions (cm ⁻¹)	Relative Intensity ^a
Uranium	776.185	7005-->19885	11
	775.419	7326-->20218	7
	778.416	620-->13463	14
	786.874	7864-->20569	9
	786.879	3800-->16505	
	838.187	7005-->18932	18
	844.538	3800-->15638	35
Thorium	781.777	10414-->23201	21
	833.045	7502-->19503	30
	841.673	0-->11877	15
Rubidium	775.765	12817-->25704	110
	775.943	12817-->25701	20
	780.023	0-->12817	30000

^a Intensity data from W.F. Meggers, C.H. Corliss, and B.F. Scribner, "Tables of Spectral-Line Intensities, Part I," NBS Monograph, 1975.

Laser-Induced Fluorescence of Yttrium Vapor

With Doppler-limited spectroscopy, it can be difficult to determine isotopic ratios if isotope shifts are not sufficiently large. We have therefore been studying the application of sub-Doppler techniques for this purpose. The sub-Doppler spectrum of gadolinium vapor was measured in an atomic beam and reported in the last quarter. The LIF spectrum of gadolinium was quite complicated due to the number of isotopes present (7), hyperfine splittings in the odd atomic mass number isotopes, and the small isotope shifts in the transition we studied. Because of these factors, a complete assignment of the spectrum was not possible. In contrast, yttrium has a much simpler spectrum. Naturally occurring yttrium is present as only a single isotope, Y-89. This isotope has a nuclear spin of 1/2. This results in fine-structure levels with $J>0$ being split into doublets by hyperfine interaction. Consequently, yttrium lines with $J>0$ and $\Delta J=0$ appear as quartets at high resolution where hyperfine splittings are resolved. There are two transitions from low-lying initial states that should be accessible to diode lasers operating in the region of 670 nm. These are the $0 \rightarrow 14949 \text{ cm}^{-1}$ and $530 \rightarrow 15246 \text{ cm}^{-1}$ transitions at 668.758 nm and 679.371 nm, respectively. We were able to excite the 668.758 nm transition with our 10 mW Toshiba (model TOLD9215) AlGaNp diode laser. We could not reach the other transition with this diode. The fluorescence excitation spectrum of yttrium in a collimated atomic beam is shown in Figure 7.

In this spectrum, peak assignments are based on the relative intensities of the two strongest peaks and the known hyperfine splitting in the lower level. Wavelength readings were made simultaneously with the recording of the spectrum with a Burleigh WA-20 wavemeter. These were of sufficient precision to establish that the separation between the first two peaks corresponded to the lower level hyperfine splitting. A least-squares fit was made to the spectrum to locate the peak positions accurately and the lower level splitting was used as an internal frequency calibration. This yielded an upper level hyperfine splitting of $180 \pm 15 \text{ MHz}$. With $J=3/2$, this gives a value of $90 \pm 8 \text{ MHz}$ for the hyperfine coupling constant A for the 14949.0 cm^{-1} level. This is the first determination of the hyperfine coupling constant for this level.

As is clear from the spectrum, we were just able to resolve some of the peaks in this spectrum. This is in part due to the particular diode laser used. The FWHM of the peaks in the spectrum is 72 MHz. This is roughly twice the width of peaks we recorded in the same atomic beam apparatus using AlGaAs diode lasers operating around 835 nm. Since the natural linewidth of the transitions studied is much smaller than this, we attribute the broader lines in this spectrum to the poorer spectral characteristics of AlGaNp diode lasers. Still, for Safeguards applications, the resolution attained with this diode laser will be sufficient for resolving U-235 from U-238 in many transitions.

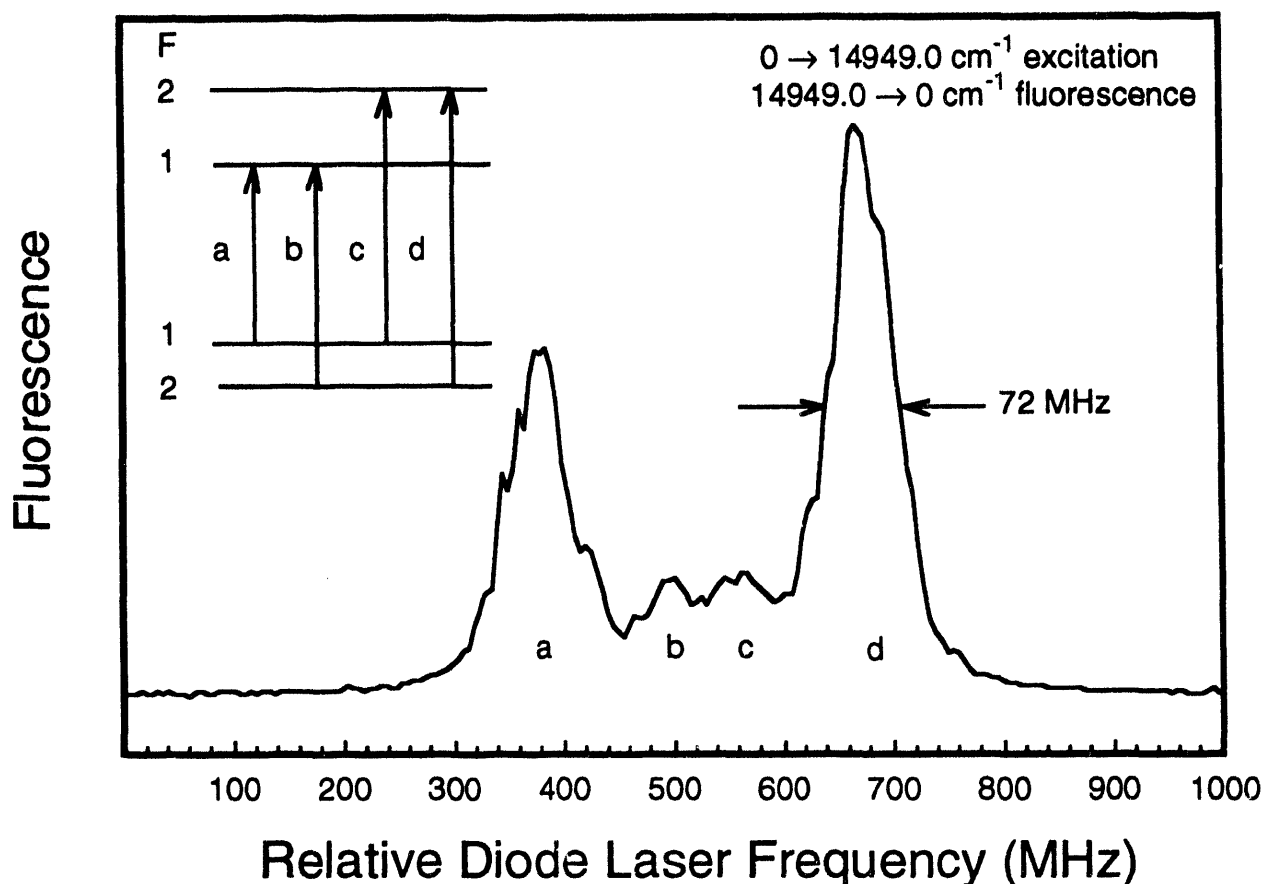


Figure 7. Fluorescence excitation spectrum of yttrium at 668.758 nm taken in a collimated atomic beam. The inset is a schematic energy level diagram showing the hyperfine splittings of the fine structure levels. F is the total angular momentum quantum number and a, b, c, d label the hyperfine transitions.

Future Studies:

Development of the diode laser system will continue. A 300 MHz confocal etalon will be ordered during the next quarter. We will initiate the design of a modified glow discharge atomizer that can be used for the quantitative analysis of actinides using high resolution spectroscopy with diode laser sources. Optogalvanic spectroscopy using diode lasers will continue and we will evaluate the merits of the technique for monitoring actinides. We will also investigate the application of diode lasers for remote spectroscopy using fiber optics.

DISTRIBUTION LIST

Mr. Edward J. McCallum, Director
Office of Safeguards and Security, SA-10
U.S. Department of Energy
Washington, D.C. 20585

Mr. David Crawford, Chief
Materials Control and Accountability Branch, SA-124
Office of Safeguards and Security
U.S. Department of Energy
Washington, D.C. 20585

Mr. Jerry Howell, Director
Field Operations Division, SA-13
Office of Safeguards and Security
U.S. Department of Energy
Washington, D.C. 20585

Dr. G. Dan Smith, Chief
Planning and Technology Development Branch, SA-134
Office of Safeguards and Security
U.S. Department of Energy
Washington, D.C. 20585

Mr. David Jones, Director
Policy, Standards, and Analysis Division, SA-12
Office of Safeguards and Security
U.S. Department of Energy
Washington, D.C. 20585

Patent Office, USDOE
Chicago Field Office
9800 South Cass Avenue
Argonne, IL 60439

USDOE-TIC
Oak Ridge National Laboratory
P.O. Box 62
Oak Ridge, TN 37830

Ms. Beth Weiser
Public Affairs & Information
Ames Laboratory
Iowa State University
Ames, IA 50011

Dr. Martin Edelson
Ames Laboratory
Iowa State University
Ames, IA 50011

Prof. T. J. Barton, Director
Ames Laboratory
Iowa State University
Ames, IA 50011

Mr. Lowell Mathison
Ames Laboratory
Iowa State University
Ames, IA 50011

Dr. C. Bingham
New Brunswick Laboratory
9800 South Cass Avenue
Argonne, IL 60439

Dr. D. C. Camp
Associate Division Leader
Lawrence Livermore National Laboratory
P.O. Box 808, L-232
Livermore, CA 94550

Mr. J. G. Douglas
Westinghouse Hanford Co.
P.O. Box 1970
Richland, WA 99352

Mr. C. E. Pietri
Physical Science Administrator
Chicago Field Office
U.S. Department of Energy
9800 South Cass Avenue
Argonne, IL 60439

A vertical stack of three abstract black and white shapes. The top shape is a horizontal rectangle divided into four vertical segments of varying widths. The middle shape is a trapezoid pointing downwards, with a diagonal line from its top-left corner to its bottom-right corner. The bottom shape is a large, solid black U-shaped block with a white rectangular cutout in its center.

四六
正一

四
五
六
七
八
九

DATA

